

- ⁸ Sondaar, P. Y., *Estudios geol., Madrid*, **17**, 209–305 (1961).
⁹ Bishop, W. W., in *Stratigraphic Succession 'versus' Calibration in East Africa* (edit. by Bishop, W. W., and Miller, J. A.), 219–246 (Scottish Academic, Edinburgh, 1972).
¹⁰ Bishop, W. W., and Pickford, M. H. L., *Nature*, **254**, 185–192 (1975).
¹¹ Bishop, W. W., Chapman, G. R., Hill, A., and Miller, J. A., *Nature*, **233**, 389–394 (1971).
¹² Hooijer, D. A., and Maglic, V. J., *Proc. K. ned. Akad. Wet.*, **76B**, 311–315 (1973).
¹³ Hooijer, D. A., and Maglic, V. J., *Zool. Verh., Leiden*, **134**, 1–34 (1974).

Distribution of hydrogen bond angles in molecular crystals

THE structures of hydrogen-bonded molecular crystals have been studied extensively, and the resulting histograms of the distributions of the O–H···O bond angles θ show maxima at approximately 15° from the linear configuration^{1–3}. At first sight this seems odd, because theoretically a linear hydrogen bond is stable^{4,5}. Kroon and Kanters³ have indicated, however, that because the number of possible hydrogen bond configurations at any value of θ is proportional to $\sin\theta$, these histograms should not be interpreted to indicate that the configuration of $\theta=15^\circ$ is, energetically, the most stable. They applied the $\sin\theta$ correction to the statistics of a series of 196 values of hydrogen bond angles in molecular crystals, and showed that the experimental distributions are not inconsistent with an assumed preference for linear hydrogen bonds.

One of us (M.H.)⁵ has calculated the potential energy function for the bending of the hydrogen bond O–H–O···O–H₂ using the method of CNDO/2, one of the semi-empirical LCAO MO SCF methods which includes all the valence electrons. We intend to show here that the histograms of Kroon and Kanters³ can be explained by Hasegawa's⁵ potential energy function.

The potential function⁵ can be represented approximately by the following quadratic form:

$$\Delta E = s\theta^2/2 \quad (1)$$

in which the linear hydrogen bond is most stable and ΔE represents the strain energy for the bending through θ degrees of the hydrogen bond. The value of the force constant, s , is estimated at 0.4 eV/rad^2 . In the case of the hydrogen-bonded water dimer, the dependence on the angle ω of the strain energy ΔE is small, so that factor is neglected here.

If it is assumed that the distribution among configurations in various molecular crystals may be approximated by a Boltzmann distribution, the distribution function $f(\theta)$ for the bending of the hydrogen bonds is represented by

$$f(\theta) = C \sin\theta \exp(-s\theta^2/2kT) \quad (2)$$

where C is the normalisation factor, k is the Boltzmann constant, and T is temperature, taken to be 300 K. The factor, $\sin\theta$, is necessary because the number of possible configurations at a given value of θ is proportional to $\sin\theta$ and the energy dependence on ω is neglected.

The histogram for the distribution of the O–H···O hydrogen bond angles can be calculated using this procedure (Fig. 2).

Figure 2 also shows Kroon and Kanters's histogram³ of 196 O–H···O hydrogen bond angles observed in molecular

Fig. 1 A bent hydrogen-bonded configuration.

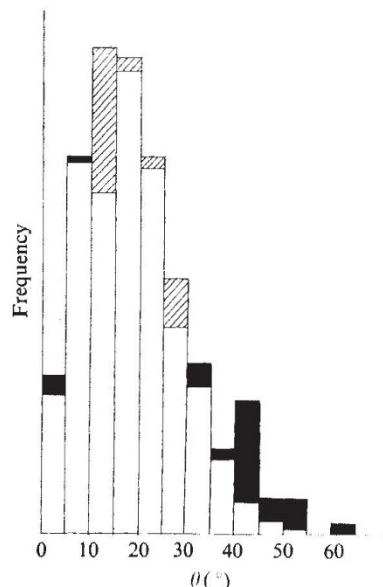
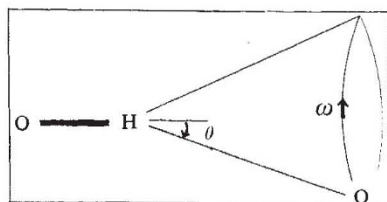


Fig. 2 The superimposed histograms of the theoretical and experimental distributions of O–H···O hydrogen bond angles. The experimental histogram is from Fig. 2 of ref. 3. Excess of experimental frequency over theoretical frequency is indicated by solid shading and excess of theoretical frequency over experimental frequency is indicated by hatching. Thus, open column indicates the amount of frequency common to both theory and experiment.

crystals. The two histograms agree quite well with each other: in our calculation the distribution shows a maximum at 14.5° , and the maximum from the molecular crystal data is approximately 15° . The slightly narrower distribution of our theoretical histogram compared with the experimental histogram may be because of the omission of the higher order terms in the right hand side of equation (1).

The hydrogen bond angle is a factor of the molecular structure and molecular arrangement in each crystal. The fact that the distribution of θ , found when the values of the hydrogen bond angle in various crystals are treated statistically, coincides with the distribution for an isolated hydrogen bonded structure, seems to suggest that the perturbation experienced by a structure of O–H···O in molecular crystals is very small.

MASAMI HASEGAWA
HARUHIKO NODA

Department of Biophysics and Biochemistry,
Faculty of Science,
University of Tokyo,
Hongo, Tokyo 113, Japan

Received December 16, 1974.

- ¹ Hamilton, W. C., and Ibers, J. A., in *Hydrogen Bonding in Solids*, 214 (Benjamin, New York, 1968).
² Ferraris, G., and Franchini-Angela, M., *Acta crystallogr.*, **B28**, 3572–3583 (1972).
³ Kroon, J., and Kanters, J. A., *Nature*, **248**, 667–669 (1974).
⁴ Hankins, D., Moskowitz, J. W., and Stillinger, F. H., *J. chem. Phys.*, **53**, 4544–4554 (1971).
⁵ Hasegawa, M., *J. phys. Soc. Japan*, **28**, 266 (1970).

Marks of unknown carbonate-decomposing organelles in cyanophyte borings

BLUE-GREEN algae are a major agent of destruction of carbonate rocks and sediments, particularly in the littoral and shallow marine environments. The organisms discussed here are endolithic, that is, the individual algal filaments reside snugly in made-to-measure tunnels of their own, excavated chemically. Data presented here suggest that much of this geologically significant bioerosion is actually caused by what may be called digestion of the mineral substance, and is not,

(Continued on page 237)

(Continued from page 212)

as previously thought, a more or less accessory effect of extracellular secretion. Endolithic cyanophytes may even turn out to be 'rock-eaters' in the true sense.

Scanning electron microscope (SEM) studies of borings of a filamentous blue-green alga of the *Hormatonema* form¹⁻³ revealed the marks of a precisely controlled excavating process, suggesting the existence of specialised boring organelles in the alga (Fig. 1). Indeed, the discovery in the cyanophytes of very refined adaptations to an endolithic mode of life should hardly be a surprising find, since these organisms, according to palaeontological data, have been boring into calcareous substrates at least since the early Ordovician (that is, for about 500 Myr) and perhaps much longer than that^{4,5}.

The boring mechanism of endolithic algae has previously been described as an extracellular dissolution process: acid or chelating fluids, released by the terminal cell, supposedly dissolve small volumes of the mineral substrate and the algal filament penetrates step by step into a tunnel formed by a sequence of small hollows^{3,6}. How the fluids are removed from the inner end of the inhabited tunnel, whether by extracellular circulation/diffusion or by metabolic uptake and intracellular transport, is not known. In the dissolution process, the micromorphology of the excavated space is determined by the solubility characteristics of the bored substrate and is thus beyond the immediate control of the organism. For example, the void space in bored calcite spar replicates the calcite rhomb⁶, and borings in dolomitic limestone may contain residual crystals of poorly soluble dolomite which has resisted the attack⁷.

The material described here derives from saline rock pools in the upper swash zone in modern beachrock west of Stazousa Point on the northern coast of Cyprus (see ref. 8). The bored rock consists in part of a coarse crystalline limestone, with optically uniform calcite crystals, several hundred micrometres across. These crystals provide excellent substrates for the study of algal borings by means of SEM.

The endolithic algae consist of dark blue filaments, about 300 μm long and 10 μm in diameter. Exposed to acid solutions the dark blue pigment turns reddish-brown, a reaction considered typical in *Hormatonema*^{3,6}. In isolated colonies consisting of a few filaments, the algae grow radially away from a common starting point whereas in crowded colonies parallel filaments grow perpendicular to the rock surface. These arrangements are consistent with the observation that algal filaments commonly repel each other and avoid connecting with other tunnels⁹.

The cavity formed by an individual filament is a fairly straight tunnel, replicating the organism. Branching of tunnels has not been observed.

As reconstructed from the microtopography of the tunnel walls, the boring process proceeds through the etching out of small grooves, about 1 μm in width and depth and 10 μm in length (Fig. 1). The wall relief increases slightly behind the terminal cell. The orientation of the grooves is approximately at right angles to the long axis of the tunnel. Interestingly enough, there are two laterally opposite sets of grooves, meeting in a zone of small pyramids. The arrangement indicates a bilateral symmetry in the boring apparatus.

The pattern of grooves shows no relationship to the internal ultrastructure or to the crystallographic parameters of the bored substrate. For example, where several tunnels run at different angles within a single calcite crystal, each tunnel has its own set of grooves which are perpendicular to the tunnel axis and are not related to the crystallographic structures of the continuous calcite lattice.

The bored rock material was collected for geological purposes and the samples were only rinsed in distilled water and air dried. Because of this crude treatment, the material

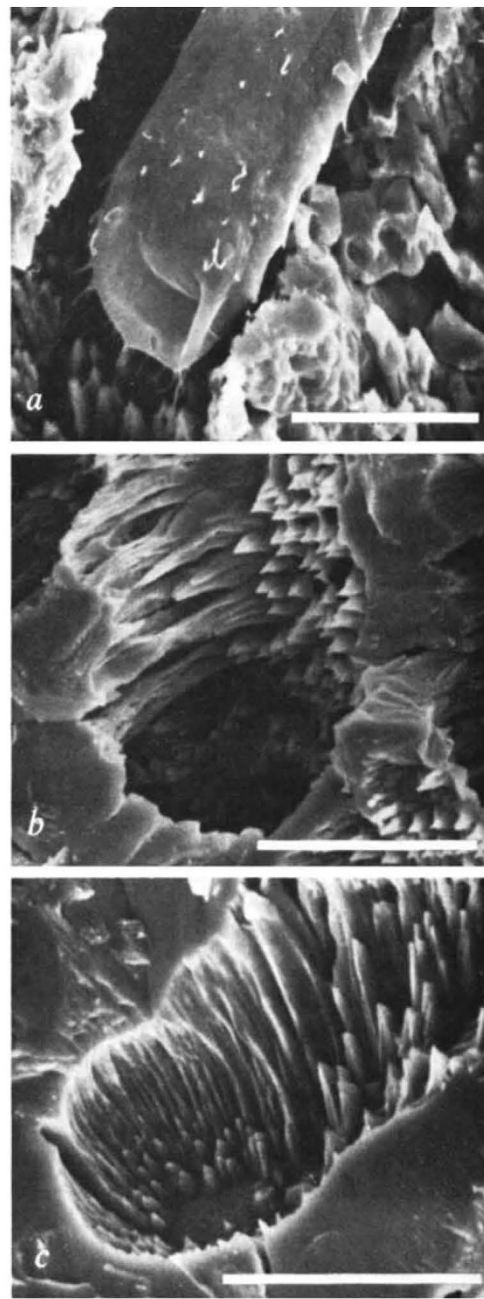


Fig. 1 Cyanophyte borings in calcite: SEM micrographs of fractured material. *a*, Penetrating tip of algal filament, slightly withdrawn from the inner end of the tunnel by shrinkage during preparation (note threads on the filament surface); *b*, oblique fracture cutting four algal tunnels in homogeneous calcite, showing one side of the bilateral pattern of grooves and the zone of small pyramids; *c*, inner end of algal tunnel with grooves and pyramids. Scale bars 10 μm .

is not suitable for a study of soft tissues, and the marks of the boring process cannot be related to specific parts of the algae. Complete algal cells, about 15 μm long and 10 μm in diameter, can obviously be ruled out as direct operators, but identification of possible boring organelles must await properly fixed and dehydrated algal material.

It is, however, interesting to observe that even in this poorly preserved material the algal filaments have a sparse coat of small threads, about 0.2 μm in diameter and 2-6 μm long (Fig. 1*a*). Similar threads have not been noted in the rich assemblages of endolithic algal filaments found in marine calcareous sediment grains^{6,9-12}. Although there is

no real evidence to suggest that the threads are boring apparatus, their presence here is probably significant.

Three conclusions can be drawn from the micromorphology of the borings. First, excavation is a chemical process, but is not straightforward extracellular dissolution on a whole-cell scale. Second external organelles, about 1 μm wide and 10 μm long, are the immediate operators. Third, the boring apparatus has a bilateral symmetry.

It can be added that, although this article considers a single species of *Hormatonema* at one locality only, I have observed similar borings in the course of SEM analyses of sedimentary carbonates from the North Sea and the Baltic Sea. It seems probable that the described mode of boring is common in the cyanophytes.

This work is part of a Marine Carbonates Programme supported by grants from the Swedish Natural Science Research Council, the Swedish Royal Academy of Science through the Hierta-Retzus Foundation, and the Magn. Bergvall Foundation.

E. TORBJORN ALEXANDERSSON

Department of Historical Geology and Palaeontology,
University of Uppsala,
Uppsala, Sweden

Received January 13, 1975.

- ¹ Le Campion-Alsumard, T., *Schweiz. Z. Hydrol.*, **32**, 552-558 (1970).
- ² Fogg, G. E., Stewart, W. D. P., Fay, P., and Walsby, A. E., *The Blue-Green Algae*, 301-302 (Academic, London, 1973).
- ³ Fogg, G. E., in *The Biology of Blue-Green Algae* (edit. by Carr, N. G., and Whitton, B. A.), 368-378 (University of California Press, Berkeley, 1973).
- ⁴ Hesseland, L., *Bull. geol. Instn. Univ. Uppsala*, **33**, 409-428 (1949).
- ⁵ Klement, K. W., and Toomey, D. F., *J. sedim. Petrol.*, **37**, 1045-1051 (1967).
- ⁶ Golubić, S., *Am. Zool.*, **9**, 747-751 (1969); in *The Biology of Blue-Green Algae* (edit. by Carr, N. G., and Whitton, B. A.), 434-472 (University of California Press, Berkeley, 1973).
- ⁷ Folk, R. L., Roberts, H. H., and Moore, C. H., *Bull. geol. Soc. Am.*, **84**, 2351-2360 (1973).
- ⁸ Alexandersson, E. T., in *The Mediterranean Sea: A Natural Sedimentation Laboratory* (edit. by Stanley, D. J.), 203-223 (Dowden, Hutchinson and Ross, Stroudsburg, Pennsylvania, 1972).
- ⁹ Alexandersson, E. T., *Bull. geol. Instn. Univ. Uppsala*, **3**, 201-236 (1972).
- ¹⁰ Margolis, S., and Rex, R. W., *Bull. geol. Soc. Am.*, **82**, 843-852 (1971).
- ¹¹ Perkins, R. D., and Halsey, S. D., *J. sedim. Petrol.*, **41**, 843-853 (1971).
- ¹² Rooney, W. S., Jr., and Perkins, R. D., *Bull. geol. Soc. Am.*, **83**, 1139-1150 (1972).

Correlation between selenium and mercury in man following exposure to inorganic mercury

THE ability of selenium compounds to modify profoundly the toxicity of both organic and inorganic mercury compounds has been demonstrated in experimental animals by Parizek and co-workers^{1,2}. The analytical data of Ganther *et al.*³ on tuna and of Koeman *et al.*⁴ on marine mammals showed that natural levels of mercury and selenium are strongly correlated. Here we report an approximately molar ratio for these elements in certain human organs following exposure to high levels of inorganic mercury.

Mercury in post-mortem samples from three groups of people—workers in the mercury mine at Idrija, Slovenia, inhabitants of the town of Idrija and a control group with no known exposure—has been analysed over the past three years^{5,6}. The study has been extended to include selenium. Although we do

not intend to discuss the mercury levels in detail, some interesting findings emerged (Table 1). Notably, the high accumulation and retention of mercury in the thyroid and pituitary; in the miners increases are of the order of a thousandfold, and in the population group about tenfold, relative to the controls. The kidney has previously been considered to be the prime accumulator of inorganic mercury, but in all eight mine workers, it ranked only third. Seven of them had been in retirement for periods up to 16 yr before death (see legend to Table 2), yet the pattern of distribution was essentially similar. It is clear that the retention of mercury in the organs with the highest accumulated levels, namely, thyroid, pituitary, kidney and brain, is very great.

In more recent post-mortem samples we have analysed both selenium and mercury to find a possible relationship between these elements in exposed humans. Both elements were analysed simultaneously by neutron activation from the same sample aliquot, using a volatilisation technique⁷ modified to allow separation and measurement of both mercury and selenium⁸. The results to date are shown in Table 2, and clearly demonstrate an approximately 1:1 molar ratio for those organs which accumulate and retain mercury strongly, namely, thyroid, pituitary, and kidney. The same effect is also seen in brain samples (Table 3), with different sections of the same brain all displaying a near molar ratio. Since selenium, as an essential trace element, will normally be present in at least typical physiological levels, whereas mercury in non-exposed persons should only approach insignificant amounts, a molar ratio will only be observed for rather elevated values. Even slightly increased mercury levels, however, seem capable of raising the selenium content; the ratio of the increments over normal levels approaches the molar ratio in many cases.

The correlation coefficient *r* between mercury and selenium in the organ group thyroid, pituitary, kidney and brain (subject T.A.) from the miners is 0.998, with two virtually identical regression equations (*r* very nearly unity) of the form

$$(\text{Se})\text{p.p.m.} = 0.41(\text{Hg})\text{p.p.m.} + 0.21 \text{ p.p.m.}$$

In molar terms, the ratio Hg-Se is 0.96:1. This ratio in the liver of marine mammals⁴ was near 1:1 in molar terms over a 2.5 decade mercury concentration range, but only a small fraction of the mercury could be recovered as methylmercury. In our work, methylmercury levels in the exposed groups, as determined by an isothermal distillation and gas chromatographic method⁹, were unremarkable, exceeding normal values only slightly. This also confirms the absence of any significant *in vivo* methylation in man.

The 1:1 molar ratio naturally suggests a direct Hg-Se linkage, though at this stage we can only speculate about the nature of the group or complex and its mode of attachment. Keeping in mind that the time between death and termination of exposure in the professionally exposed subjects varied greatly, it seems that the effect is both accumulative (as in the case of marine mammals and tuna) and retentive. This emphasises the strength of the Hg-Se interaction and suggests their removal from biological turnover. The coaccumulation of selenium observed in this study is certainly not the result of coexisting high levels of

Table 1 Average mercury content with standard deviation of human organs in p.p.m. fresh weight

Group	Thyroid	Pituitary	Kidney	Liver	Lung	Brain
Mercury mine workers	35.2 ± 28.5 (8)	27.1 ± 14.9 (7)	8.4 ± 4.9 (8)	0.26 ± 0.25 (8)	1.11 ± 0.89 (5)	0.70 ± 0.64* (6)
	7.8 - 101	13.8 - 64.3	2.3 - 18.5	0.04 - 0.79	0.13 - 1.58	0.18 - 1.50*
Idrija population	0.70 ± 0.45† (10)	0.46 ± 0.54 (11)	0.66 ± 1.13 (11)	0.107 ± 0.059 (11)	0.127 ± 0.100 (10)	0.038 ± 0.045† (9)
	0.03 - 3.6	0.02 - 1.76	0.03 - 4.0	0.02 - 0.21	0.005 - 0.24	0.002 - 0.11
Non-exposed controls	0.030 ± 0.037 (16)	0.040 ± 0.026 (6)	0.14 ± 0.16 (7)	0.030 ± 0.017 (8)	—	0.0042 ± 0.0026 (5)
	0.003 - 0.13	0.007 - 0.064	0.01 - 0.37	0.01 - 0.05	—	0.001 - 0.007

Figures in parentheses refer to the number of subjects analysed, ranges are given below.

* Excluding T.A.; see Tables 2 and 3. † Excluding P.M.